

# Density of States and Magnetic Correlations at a Metal-Mott Insulator Interface

M. Jiang<sup>1,2</sup>, G.G. Batrouni,<sup>3,4</sup> and R.T. Scalettar<sup>1</sup>

<sup>1</sup>*Physics Department, University of California, Davis, California 95616, USA*

<sup>2</sup>*Department of Mathematics, University of California, Davis, California 95616, USA*

<sup>3</sup>*INLN, Université de Nice-Sophia Antipolis, CNRS; 1361 route des Lucioles, 06560 Valbonne, France and*

<sup>4</sup>*Institut Universitaire de France*

The possibility of novel behavior at interfaces between strongly and weakly correlated materials has come under increased study recently. In this paper, we use determinant Quantum Monte Carlo to determine the inter-penetration of metallic and Mott insulator physics across an interface in the two dimensional Hubbard Hamiltonian. We quantify the behavior of the density of states at the Fermi level and the short and long range antiferromagnetism as functions of the distance from the interface and with different interaction strength, temperature and hopping across the interface. Induced metallic behavior into the insulator is evident over several lattice spacings, whereas antiferromagnetic correlations remain small on the metallic side. At large interface hopping, singlets form between the two boundary layers, shielding the two systems from each other.

PACS numbers: 71.10.Fd, 71.30.+h, 02.70.Uu

## I. INTRODUCTION

Over the last decade, advances in synthesis techniques have made possible the construction of well-defined interfaces involving strongly correlated materials, notably transition metal oxides<sup>1-4</sup>. Indeed, the early discovery that the interface between two insulating oxides, LaAlO<sub>3</sub> and SrTiO<sub>3</sub> is a high-mobility two dimensional conductor<sup>5</sup> or even a superconductor<sup>6</sup> has emphasized that novel physics can arise at such boundaries, beyond a simple interpolation between materials properties on either side. Subsequently, numerous heterostructure interfaces have been shown to exhibit unique phenomena that are not present in their bulk constituents. In particular, Munakata *et al.* presented a subtle proximity effect that arises between a normal metal and an antiferromagnetic Mott insulator, which can be understood in the framework of Ruderman-Kittel-Kasuya-Yoshida (RKKY) interactions<sup>3</sup>.

Advances in characterization techniques are also expanding the horizon of the field. It was shown recently that, by setting up a standing wave of the incident X-rays and adjusting the position where the intensity is peaked inside the sample, one can measure electronic excitations as a function of location in the sample. This standing wave angle resolved photoemission spectroscopy (SW-ARPES)<sup>7</sup> method allows a depth selective probe of buried layers and interfaces, and hence the construction of chemical and electronic structure profiles within the sample.

Various numerical methods have been employed to model qualitative features of these experiments. Early attempts include the study of LaAlO<sub>3</sub> and SrTiO<sub>3</sub> systems in which the electric fields arising from the La<sup>3+</sup>/Sr<sup>2+</sup> charge difference and the on-site interactions are treated within the Hartree-Fock approximation<sup>8</sup>. A metallic interface between band and Mott insulators in a quasi-one-dimensional lattice was explored with the Lanczos method<sup>9</sup>. Important insights into electronic

properties at interfaces have also been gained by dynamical mean field theory (DMFT)<sup>10</sup>. For example, it has been suggested that the Kondo effect governing the interface between metal and Mott insulator is inefficient so that Mott insulators are impenetrable to the metal<sup>11</sup>. More specifically, the quasiparticle weight decays as  $1/x^2$  with distance  $x$  from the metal, but the prefactor of this decay was found to be very small. Zenia *et al.*, however, emphasized that even a small proximity effect can induce density of states to open up a metallic channel inside an insulator sandwiched between to metals at sufficiently low temperatures<sup>12</sup>, leading to perfect conductance. This Fermi liquid is “fragile”: finite temperature, disorder, or frequency rapidly return the behavior to that of a conventional N-I-N junction. Possible device applications were suggested as a consequence of this sensitivity.<sup>1-4</sup> In a related work<sup>13</sup>, a Gutzwiller approximation approach was extended to inhomogeneous systems. The decay length of the exponential fall-off of the penetration of metallic character into the insulator region was shown to diverge as the metal-insulator transition is approached.

A further interesting set of studies involves the dynamical response of strongly correlated systems with an interface, for example the possibility of the suppression of charge transport, current rectification, and the behavior of holon-doublon pairs, which are important for devices<sup>14</sup>. So far, such dynamic phenomena have been explored primarily for one-dimensional systems, where time-dependent Hartree Fock<sup>15</sup> and density-matrix renormalization group (DMRG) methods are especially effective<sup>16</sup>.

In this paper, we address the metal-insulator interface problem by using determinant Quantum Monte Carlo (DQMC)<sup>17,18</sup>, a numerically exact approach, to treat correlated electron models. Here we focus on an inhomogeneous Hubbard model on a single two dimensional lattice divided by a linear interface in two regions, one weakly correlated (with  $U = 0$ ), and one at intermediate coupling (with  $U$  non-zero). The chemical potential

is chosen to maintain particle-hole symmetry, so that all sites of the lattice are on average half-filled. This choice avoids the fermion sign problem<sup>19</sup> and enables the evaluation of magnetic correlations and the density of states at low temperature.

Such DQMC simulations are at present limited to lattices of 400 – 1000 sites (depending on the interaction strength and temperature). By focussing on a linear interface in a 2D lattice, we are able to explore systems with a fairly large linear extent. Most of our results will be for  $20 \times 20$  lattices. This enables us, for example, to evaluate the penetration depth across the boundary, since the interface effects have sufficient room to heal before the lattice edge. The behavior of the Hubbard model across a planar interface in a 3D material on systems of smaller linear extent has been explored by Euverte *et al*<sup>20</sup>. The key finding is that up to an interface hopping  $V$  which is on the order of the bulk hybridization  $t$ , the effects of the interface can extend well past the two layers immediately at the interface. That is, the interface affects properties 3 – 4 layers deep on both the strongly and weakly correlated sides of the boundary. When  $V \geq 2t$ , however, there is a return to the values characteristic of decoupled materials with  $V = 0$ . This “revival” of magnetic order on the insulating side is driven by the formation of singlets between fermions on the two layers immediately adjacent to the interface which acts to decouple the two materials.

This paper is organized as follows: In section II we explicitly write down the Hamiltonian and provide a very brief overview of DQMC. Section III focuses on the magnetic properties of the 2D lattice with a linear interface, both the near-neighbor spin correlation and the structure factor. Here the interaction strength  $U$  and temperature  $T$  are varied at fixed interface hopping  $V$ . The key result is a determination of the penetration depth as a function of  $T$  and  $U$ . Section IV extends these results to the density of states. Section V examines the variation with  $V$ , and Section VI summarizes our results.

## II. MODEL AND METHODOLOGY

We consider the two-dimensional Hubbard model

$$\begin{aligned} \hat{H} = & -t \sum_{\langle ij \rangle, L, \sigma} (c_{iL\sigma}^\dagger c_{jL\sigma} + h.c.) - \mu \sum_{i, L, \sigma} n_{iL\sigma} \\ & - \sum_{i, \langle LL' \rangle, \sigma} t_{LL'} (c_{iL\sigma}^\dagger c_{iL'\sigma} + h.c.) \\ & + \sum_{i, L} U_L (n_{iL\uparrow} - \frac{1}{2})(n_{iL\downarrow} - \frac{1}{2}) \end{aligned} \quad (1)$$

Here  $c_{iL\sigma}^\dagger (c_{iL\sigma})$  are fermionic creation (destruction) operators of spin  $\sigma$  at site  $i$  in line  $L$ . While  $i, L$  can also be regarded as the  $x$  and  $y$  site labels  $i_x, i_y$ , the current notation emphasizes the broken rotational symmetry

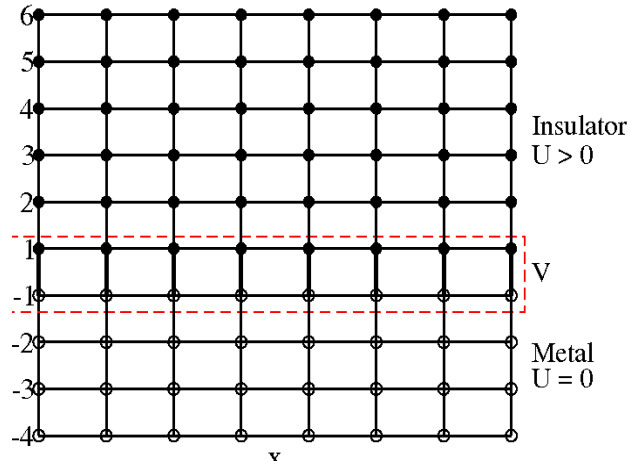


FIG. 1: (color online) Geometry of the two-dimensional lattice with a one-dimensional interface (dashed red box). The metallic lines (negative  $L$ ) have  $U = 0$  while the insulating lines (positive  $L$ ) have  $U \neq 0$ . The lattice has periodic boundary conditions in the  $x$  direction and open boundary conditions in the  $L$  direction.  $V$  denotes the hopping/hybridization (heavy lines) across the interface. We adopt the lattice size  $N = 20 \times 20$  throughout the paper, unless otherwise indicated.

(the interface is parallel to the  $x$  axis). Our labeling convention is  $L = \dots -3, -2, -1$  for the  $U = 0$  lines and  $L = 1, 2, 3, \dots$  for the  $U \neq 0$  lines, so that the interface connects  $L = \pm 1$ .  $t$  and  $t_{LL'}$  are the intra and inter-line nearest-neighbor hoppings.  $t_{LL'} = t$  except at the interface where  $t_{-1,1} = V$ . The geometry is shown in Fig. 1.

The DQMC approach provides an exact solution to the finite temperature properties of  $H$  by decoupling the interaction term  $U$  through the introduction of an auxiliary Hubbard-Stratonovich (HS) field. The resulting action is quadratic in the fermion operators, so that the trace over those coordinates can be performed, leaving determinants (one for spin up and one for spin down) of matrices whose dimensions are the spatial lattice size, and whose entries depend on the HS field. The auxiliary field is sampled stochastically, and the values of the up and down spin fermion Green’s function for the configurations generated are used to construct the various observables. The CPU time for the algorithm scales as the cube of the lattice size and linearly<sup>21</sup> with inverse temperature  $\beta$ .

At low temperatures, the fermion determinants can become negative, precluding their use as a probability for sampling the HS field. To avoid this “sign problem”, we consider the half-filled case,  $\mu = 0$ . Here particle-hole symmetry (PHS) implies that  $\langle n_{iL\sigma} \rangle = 0.5$  for all temperatures and interaction strengths, even if  $U_L$  vary spatially with  $L$  and the hybridizations are not all equal. PHS can also be used to demonstrate that the up and down spin determinants, although they can individu-

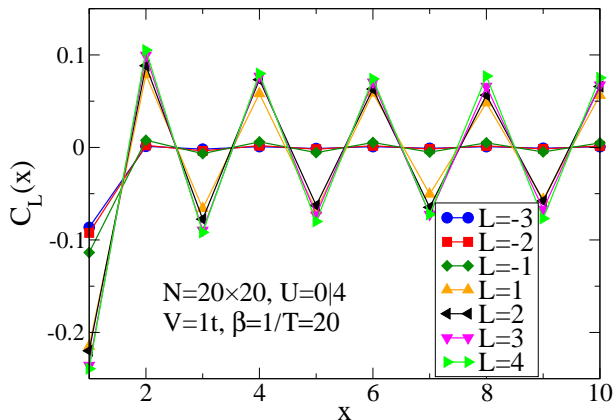


FIG. 2: (color online) Spin correlation  $C_L(x) = \langle S_{i,L} S_{i+x,L} \rangle$  as a function of separation  $x$  for different lines  $L$ . Diminishing antiferromagnetism of the insulator adjacent to the interface is shown. The induced antiferromagnetic long-range orders in the metallic region are evident in spite of their weaknesses.  $U = 0|4$  denotes the interface setup.

ally become negative, always have the same sign. As a consequence, their product is always positive, allowing the study of the low temperature behavior at the metal-insulator interface.

### III. MAGNETIC PROPERTIES

We gain quantitative information concerning the spin correlations in different lines by measuring the spin correlation  $C_L(x) = \langle S_{i,L}^- S_{i+x,L}^+ \rangle$ , with  $S_{i,L}^- = c_{i\uparrow} c_{i\downarrow}^\dagger$ , parallel to the interface. Figure 2 shows that antiferromagnetism in the insulating layer  $L = 1$  immediately adjacent to the metal is diminished by 20-30% relative to larger positive  $L$  which are deeper in the Mott insulator. Data are shown for boundary hybridization  $V = t$  and interaction  $U = 4t$  in the insulator. Despite a somewhat smaller amplitude, the correlations in  $L = 1$  appear to remain long ranged. Induced antiferromagnetic long-range order<sup>22</sup> in the metallic region is also evident, although its amplitude is an order of magnitude smaller than that on the insulating side.

Compact information on the antiferromagnetic long-range order for each line  $L$  can be obtained by measuring the antiferromagnetic (AF) structure factor,

$$S_{AF}(L) = \frac{1}{N} \sum_x (-1)^x \cdot C_L(x) \quad (2)$$

where  $N$  is the linear lattice size. Figure 3 illustrates the  $L$ -dependent AF structure factor for different correlation strengths  $U$  and temperatures  $T$ . The smooth penetration of antiferromagnetic order into the metal and the diminishing AF order in the insulator are clearly seen. As might be expected, the induced long range AF order

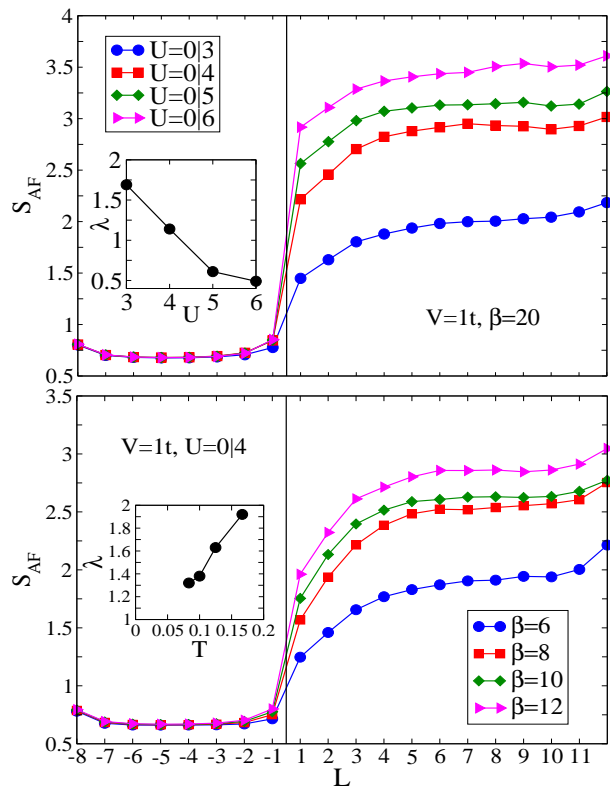


FIG. 3: (color online) AF structure factor  $S_{AF}(L)$  in each line  $L$  for different correlation strengths  $U$  and temperatures  $T$ . The smooth penetration of antiferromagnetic order into the metal and the diminishing AF order in the insulator are clearly seen. Fitting  $S_{AF}(L)$  to a hyperbolic function<sup>23</sup>,  $a \tanh L/\lambda + b$  allows the extraction of a penetration length  $\lambda$ , shown in the insets.  $\lambda$  decreases with larger correlation  $U$  and lower temperature  $T$ . Further information

in the metal adjacent to the interface is stronger for correlated insulator with larger<sup>24</sup> on-site repulsion  $U$  (Fig. 3a) and/or lower temperature (Fig. 3b). The overall magnitude of  $S_{AF}$  in the metal is rather small, consistent with the small real-space correlations in Fig. 2. The results of Figs. 2,3 are rather different from previous work of Sherman *et al.*<sup>25</sup> which found that the antiferromagnetic order can penetrate into the metal to a depth of ten lattice spacings, but are consistent with the shorter range effects described in<sup>11,12</sup>. Figure 3 indicates that by layer  $L = -3$  the influence of the contact with the insulator is minimal.

On the other hand, we find that contact with the metal has a substantially greater effect on the insulator. Here the “Kondo proximity effect” diminishes the long range AF order of the insulating lines adjacent to the interface. This tendency to paramagnetism competes with the long range order induced by the exchange energy  $J \sim t^2/U$  deep in the insulator (Fig. 3a). To quantify the proximity effects, we fit the curves of  $S_{AF}(L, U, T)$  with the hyperbolic form  $S_{AF}(L, U, T) = a \tanh L/\lambda + b$ . The penetration depth  $\lambda$  decreases with larger correla-

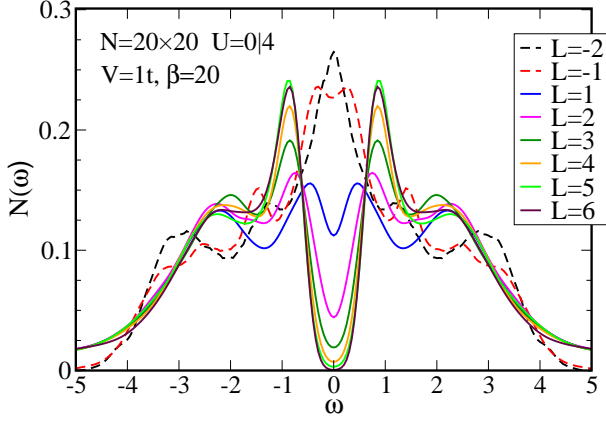


FIG. 4: (color online) The  $L$  dependence of the density of states  $N(\omega)$  shows the evolution of the spectral properties across the metal-insulator interface. Lines of sites within the Mott insulator ( $L > 0$  have nonzero  $U$ ) are characterized by the presence of Kondo resonance peaks split by antiferromagnetic order at half-filling. However this AF gap between the two peaks is dramatically weakened as  $L \rightarrow 1$ . On the other hand, the densities of states associated with lines of sites on the metallic side of the interface show little effect of contact with the insulator. Even for the line  $L = -1$  most immediately adjacent to the boundary there is only a small dip in  $N(\omega)$  at  $\omega = 0$ .

tion  $U$ . Interestingly,  $\lambda$  increases at higher temperature. It is possible that raising  $T$  weakens the magnetic order in the insulator, thereby enhancing the effects of the contact with the metal.

#### IV. DENSITY OF STATES

One criterion to distinguish metal from insulator is the single particle density of states, which can be extracted from the local imaginary-time dependent Green's function  $G_L(\tau) = \sum_{i\sigma} T c_{iL\sigma}(\tau) c_{iL\sigma}^\dagger(0)$  from

$$G_L(\tau) = \int_{-\infty}^{\infty} d\omega \frac{e^{-\omega\tau}}{e^{-\beta\omega} + 1} N_L(\omega) \quad (3)$$

and using the maximum entropy method<sup>26</sup>. The density of states is probed experimentally with photoemission spectroscopy. In a translationally invariant system one often also calculates the momentum dependent spectral function  $A(k, \omega)$ , measured in angle-resolved photoemission spectroscopy (ARPES).

As mentioned in the introduction, a dramatic experimental achievement in the past few years has been the development of standing wave ARPES<sup>7</sup> which has enabled the probing of strong correlation effects layer by layer in a sample. Here we make some predictions for possible features to be seen in SWARPES by obtaining the row dependent single particle density of states. As

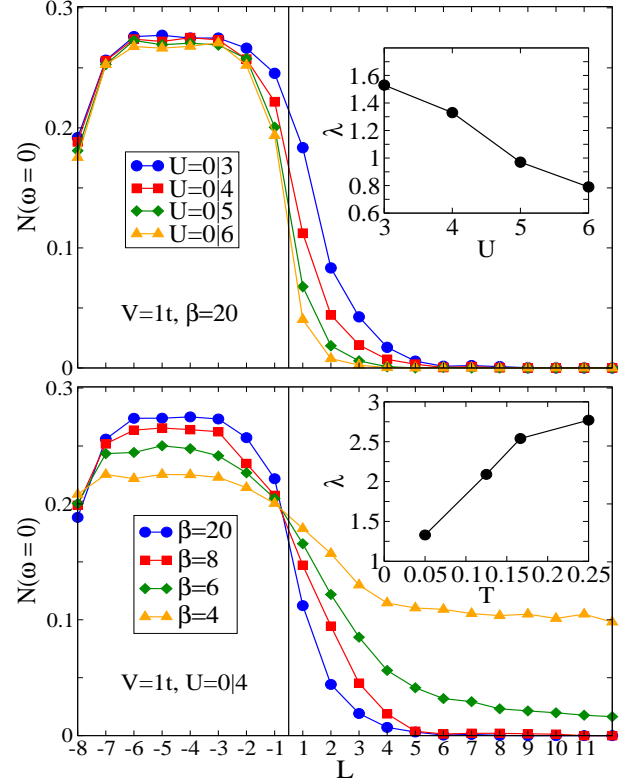


FIG. 5: (color online)  $L$ -dependent density of states for different on-site repulsions  $U$  and temperatures  $T$ . The smooth penetration of metallicity into the insulator and diminished metallic behaviors in the metal are clearly seen. Similar to Fig. 3, we employ a hyperbolic fitting function and extract a penetration depth  $\lambda$  (insets), which we find decreases with larger correlation  $U$  and increases with higher temperature  $T$ .

with the row-by-row magnetic correlations,  $N_L(\omega)$  shown in Fig. 4 characterizes the penetration of metallicity into the insulator. Kondo proximity effects are evident in the evolution of  $N_L(\omega)$ . Figure 4 shows that the insulating lines for  $L = 6, 5, 4$ , relatively far from the interface, are characterized by the presence of a Kondo resonance peak split by antiferromagnetic order at half-filling. However as the interface is approached for  $L = 3, 2, 1$  the gap is increasingly filled in, evidence of the coupling to the metallic half of the lattice. Meanwhile the metallic line ( $L = -1$ ) immediately adjacent to the interface shows some influence of the boundary, albeit a rather small one: the central peak at  $\omega = 0$  shows a slight dip. This is completely gone for  $L = -2$ . Evidently the metallic behavior of  $N(\omega)$  penetrates much further into the insulator than the insulating physics does into the metal.

Further information on the spectral weight at Fermi level  $N_L(U, T)|_{\omega=0}$  as a function of on-site repulsion  $U$  and temperature  $T$  is shown in Fig. 5. The penetration of metallic behavior into the insulator and, conversely, the diminished spectral weight at the Fermi surface in the metal are clearly seen. Similar to Fig. 3, we adopt a hyperbolic function for fitting. The resulting penetration



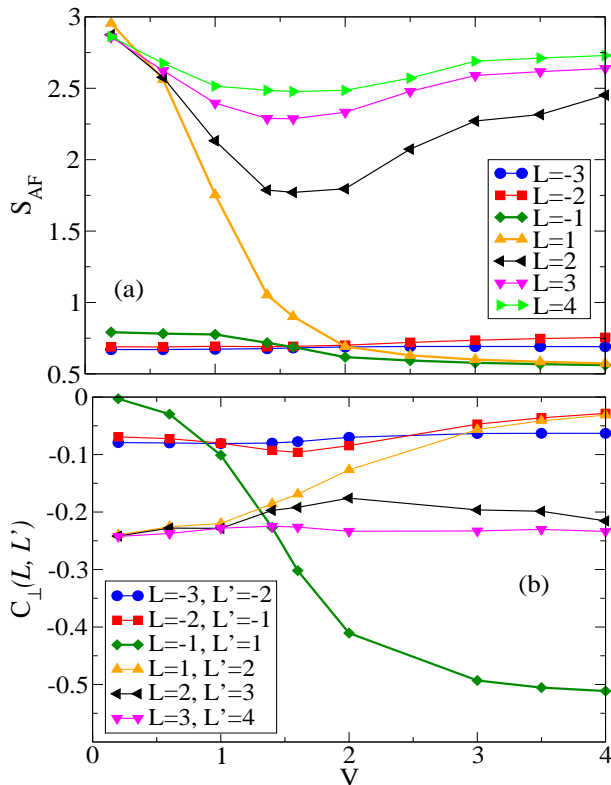


FIG. 6: (color online) (a) Evolution of the antiferromagnetic (AF) structure factors  $S_{AF}(L)$  with interface hybridization  $V$ . Except the line of sites  $L = 1$ , adjacent to the metal,  $S_{AF}(L > 1)$  exhibits a nontrivial revival with increasing the  $V$ . We attribute this affect to singlet formation at the metal-insulator interface which leaves the lines  $L > 1$  decoupled from the metal. (b) Further evidence of the strong magnetic coupling across the interface.  $U = 0|4, \beta = 10$ .

depths  $\lambda$  are given in the inset, and decrease with larger correlation  $U$  and lower temperature  $T$ .

## V. EFFECT OF VARIATION OF INTERFACE HOPPING

We show in Fig. 6 the evolution of the line dependent AF structure factors  $S_{AF}(L)$  with interface hopping  $V$ . As expected, all lines  $L > 0$  with nonzero on-site repulsion  $U = 4$  have large  $S_{AF}$  when the metal and insulator are decoupled ( $V = 0$ ). With increasing hybridization all  $S_{AF}(L > 0)$  initially decrease. The most dramatic feature in Fig. 6(a) is the different behaviors of  $S_{AF}(L = 1)$  and  $S_{AF}(L > 1)$ . In the line  $L = 1$ , adjacent to the metal-insulator interface,  $S_{AF}(L = 1)$  monotonically decreases with  $V$ . However,  $S_{AF}(L > 1)$  show nontrivial revivals with increasing  $V$  and ultimately recover to values characteristic of the decoupled case  $V = 0$  when there is no contact with the metal whatsoever. This behavior of  $S_{AF}(L)$  is qualitatively similar to the multi-layer metal-insulator interface in the three-dimensional Hub-

bard model<sup>20</sup>, and can be attributed to “singlet” formation at the metal-insulator interface, which both suppresses  $S_{AF}(L = 1)$  and also leaves the remaining lines  $L > 1$  decoupled from the metal.

The “metallic” line structure factors  $S_{AF}(L)$  retain their small values for the entire range of  $V$ . As with the real space spin correlation functions, there is a greater effect of the metal on the insulator (suppressing magnetic order) than of the insulator on the metal (inducing magnetic order).

Figure 6(b) provides further evidence of the strong magnetic coupling across the interface. The dominant feature is the rapid increase of antiferromagnetic correlation across the metal-insulator interface  $C_{\perp}(L = -1, L' = 1)$  as increasing the hopping  $V$ . Note also that magnetic correlation  $C_{\perp}(L = 1, L' = 2)$  become smaller with larger hopping  $V$  due to the “singlet” formation at the interface  $L = -1, 1$ .

## VI. CONCLUSION

We have used the numerically exact finite-temperature determinant Quantum Monte Carlo (DQMC) method to study a metal-insulator interface in a two-dimensional square lattice. By investigating the long-range antiferromagnetic order and density of states, we demonstrated that the metallic behavior penetrates into the insulator for several lattice spacings, with a penetration depth  $\lambda$  which decreases with increasing on-site repulsion,  $U$ , on the insulator side of the interface.  $\lambda$  is also (somewhat more weakly) temperature dependent, decreasing as  $T$  is lowered towards the critical temperature  $T_c = 0$  for long range magnetic order on the insulating side. The penetration length  $\lambda$  thus shows an opposite temperature dependence to that of the spin correlation length,  $\xi$ , which grows as  $T$  is lowered.

The insulator-induced antiferromagnetic long-range order in the metal is predominantly limited to the line immediately adjacent to the interface. That is, magnetic characteristics of strong correlation appear to penetrate less deeply into the metallic side of an interface than does weak correlation physics penetrate into the insulator. This is consistent with previous results for a planar interface in a 3D lattice<sup>20</sup>. We note, however, that in the 3D geometry, the effect of the contact with the insulator on the in-plane conductivity  $\sigma$  in the  $U = 0$  half of the lattice can extend beyond the contact layer. This is consistent with our results for the density of states at the Fermi level  $N(\omega = 0)$ , which are shifted from their  $U = 0$  values for layer  $L = -2$  in addition to layer  $L = -1$ .

In the past several years, studies of the effect of spatially varying densities and interaction strengths have been motivated by experiments on trapped atomic gases<sup>27–30</sup>. In such systems the spatial variation, eg a quadratic confining potential  $V_{\text{trap}}(r) = V_T(r/l)^2$ , has an explicit length scale  $l$ . This complicates the determination of intrinsic length scales associated with the

response of the interacting fermions themselves. Our choice here of a sharp (scale free) interface between metal and insulator ( $U_L = 0, L = -1, -2, -3, \dots$  and  $U_L = U > 0, L = 1, 2, 3, \dots$ ) allows us to attribute the lengths characterizing the relaxation of properties on either side of the interface solely to the fermionic correlations. This choice is, of course, also more appropriate to the solid state context of a sharp interface between two materials.

One further motivation to study the metal-insulator interface is its close relation to the question of “orbitally selective Mott transitions” (OSMT)<sup>31–36</sup>. Here the central question is whether orbitals with different degree of electronic correlation, coupled together by interorbital hybridization, necessarily undergo the Mott transition simultaneously. The layer index ‘L’ in the Hamiltonian considered in this paper bears a formal similarity to the orbital degree of freedom in the OSMT, although of course the details of the coupling via hybridization are rather different in the two cases. It is evident from our data that a layer which shows the hallmarks of an antiferromagnetic Mott insulator can coexist with layers which have the characteristic behavior of a paramagnetic metal. That such coexistence is possible is similar to the

conclusion ultimately reached in numerical studies of the OSMT.

In this paper, the density of states and magnetic correlations near an interface between  $U = 0$  and  $U \neq 0$  regions have been found to be more or less smooth interpolations between the bulk metal and Mott insulator. On the other hand, Quantum Monte Carlo simulations have observed novel phases<sup>37</sup> such as spin liquids, to arise in models where the energy scales are poised at the boundary between a semi-metal and an antiferromagnet. An interesting extension of the present work would be, therefore, to bring such more general regions into contact and study the properties at the interface.

## VII. ACKNOWLEDGEMENTS

We acknowledge support from the National Science Foundation under grant NSF-PIF-1005502. This work was also supported under ARO Award W911NF0710576 with funds from the DARPA OLE Program and by the CNRS-UC Davis EPOCAL LIA joint research grant. We are grateful to Bo Deans for useful input.

- 
- <sup>1</sup> P. Zubko, S. Gariglio, M. Gabay, P. Ghosez, and J.M. Triscone, *Annu. Rev. Condens. Matter Phys.* **2**, 141 (2011), and references therein.
  - <sup>2</sup> J. Mannhart and D.G. Schlom, *Science* **327**, 1607 (2010).
  - <sup>3</sup> K. Munakata, T.H. Geballe, and M.R. Beasley, *Phys. Rev. B* **84**, 161405(R) (2011).
  - <sup>4</sup> J. W. Freeland, J. Chakhalian, A.V. Boris, J.M. Tonnerre, J.J. Kavich, P. Yordanov, S. Grenier, P. Zschack, E. Karapetrova, P. Popovich, H. N. Lee, and B. Keimer, *Phys. Rev. B* **81**, 094414 (2010).
  - <sup>5</sup> A. Ohtomo, D. A. Muller, J.L. Grazul, and H.Y. Hwang, *Nature* **419**, 378 (2002).
  - <sup>6</sup> S. Thiel, G. Hammerl, A. Schmehl, C.W. Schneider, and J. Mannhart, *Science* **313**, 1942 (2006).
  - <sup>7</sup> A.X. Gray, C. Papp, B. Balke, S.-H. Yang, M. Huijben, E. Rotenberg, A. Bostwick, S. Ueda, Y. Yamashita, K. Kobayashi, E.M. Gullikson, J.B. Kortright, F.M.F. DeGroot, G. Rijnders, D.H.A. Blank, R. Ramesh, C.S. Fadley, *Phys. Rev. B* **82**, 205116 (2010).
  - <sup>8</sup> S. Okamoto and A. J. Millis, *Nature (London)* **428**, 630 (2004); *Phys. Rev. B* **70**, 075101 (2004).
  - <sup>9</sup> S.S. Kancharla and E. Dagotto, *Phys. Rev. B* **74**, 195427 (2006).
  - <sup>10</sup> S. Okamoto and A. J. Millis, *Phys. Rev. B* **70**, 241104(R) (2004).
  - <sup>11</sup> R. W. Helmes, T. A. Costi, and A. Rosch, *Phys. Rev. Lett.* **101**, 066802 (2008).
  - <sup>12</sup> H. Zenia, J. K. Freericks, H. R. Krishnamurthy, and T. Pruschke, *Phys. Rev. Lett.* **103**, 116402 (2009).
  - <sup>13</sup> G. Borghi, M. Fabrizio, and E. Tosatti, *Phys. Rev. B* **81**, 115134 (2010).
  - <sup>14</sup> Luis G.G.V. Dias da Silva, K.A. Al-Hassanieh, A.E. Feiguin, F.A. Reboredo, and E. Dagotto *Phys. Rev. B* **81**, 125113 (2010).
  - <sup>15</sup> S. Yonemitsu, N. Maeshima, and T. Hasegawa, *Phys. Rev. B* **76**, 235118 (2007).
  - <sup>16</sup> S. R. White and A. E. Feiguin, *Phys. Rev. Lett.* **93**, 076401 (2004).
  - <sup>17</sup> R. Blankenbecler, D.J. Scalapino, and R.L. Sugar, *Phys. Rev. D* **24**, 2278 (1981).
  - <sup>18</sup> S.R. White, D.J. Scalapino, R.L. Sugar, E.Y. Loh, Jr., J.E. Gubernatis, and R.T. Scalettar, *Phys. Rev. B* **40**, 506 (1989).
  - <sup>19</sup> E. Y. Loh, Jr., J. E. Gubernatis, R. T. Scalettar, S. R. White, D. J. Scalapino, and R. L. Sugar, *Phys. Rev. B* **41**, 9301 (1990).
  - <sup>20</sup> A. Euverte, F. Hebert, S. Chiesa, R.T. Scalettar, and G.G. Batrouni, *Phys. Rev. Lett.* **108**, 246401 (2012).
  - <sup>21</sup> The linear scaling in  $\beta$  is restricted to cases when the matrix condition number does not become overly large: At large interaction strengths  $U$  the necessity of recomputing the green’s function from scratch due to numerical instabilities can introduce  $\beta^2$  terms. These can also arise in computation of the imaginary time dependent Greens function.
  - <sup>22</sup> ‘Long range order’ might be a bit of a misnomer. Although the correlations remain non-zero at long distances, it is likely this reflects an imposed order from the external contact with the insulator, as opposed to order mediated through the metallic layer itself.
  - <sup>23</sup> The increase of  $S_{AF}$  at the two open boundaries is left out of our fitting. This phenomenon where “surface” magnetic correlations are larger than the “bulk”, despite the smaller number of neighbors, occurs because of the reduced quantum fluctuations (hopping) at the “surface”. See, for example, F. Zhang, S. Thevuthasan, R.T. Scalettar, R.R.P. Singh, and C.S. Fadley, *Phys. Rev. B* **51**, 12468

- (1995), and references therein.
- <sup>24</sup> Actually, magnetic correlations in the Hubbard model peak at  $U \sim 8t$ , ultimately declining when  $U$  becomes very large owing to the decreasing exchange energy  $J \sim t^2/U$  at large  $U$ .
  - <sup>25</sup> A. Sherman and N. Voropajeva, *Int. J. Mod. Phys. B* **24**, 979 (2010).
  - <sup>26</sup> J.E. Gubernatis, M. Jarrell, R.N. Silver, and D.S. Sivia, *Phys. Rev. B* **44**, 6011 (1991); A. W. Sandvik, *Phys. Rev. B* **57**, 10287 (1998).
  - <sup>27</sup> D. Jaksch, C. Bruder, J.I. Cirac, C.W. Gardiner, and P. Zoller, *Phys. Rev. Lett.* **81**, 3108 (1998).
  - <sup>28</sup> G.G. Batrouni, V. Rousseau, R.T. Scalettar, M. Rigol, A. Muramatsu, P.J.H. Denteneer, and M. Troyer, *Phys. Rev. Lett.* **89**, 117203 (2002).
  - <sup>29</sup> T. Stöferle, H. Moritz, K. Günter, M. Köhl, and T. Esslinger, *Phys. Rev. Lett.* **96**, 030401 (2006).
  - <sup>30</sup> J.K. Chin, D.E. Miller, Y. Liu, C. Stan, W. Setiawan, C. Sanner, K. Xu, and W. Ketterle, *Nature (London)* **443**, 961 (2006).
  - <sup>31</sup> A. Liebsch, *Phys. Rev.* **B70**, 165103 (2004).
  - <sup>32</sup> R. Arita and K. Held, *Phys. Rev.* **B72**, 201102(R) (2005).
  - <sup>33</sup> A. Koga, N. Kawakami, T.M. Rice, and M. Sigrist, *Phys. Rev. Lett.* **92**, 216402 (2004).
  - <sup>34</sup> M. Ferrero, F. Becca, M. Fabrizio, and M. Capone, *Phys. Rev.* **B72**, 205126 (2005).
  - <sup>35</sup> L. de'Medici, A. Georges, and S. Biermann, *Phys. Rev.* **B72**, 205124 (2005).
  - <sup>36</sup> C. Knecht, N. Blumer, and P.G.J. van Dongen, *Phys. Rev.* **B72**, 081103(R) (2005).
  - <sup>37</sup> An early example of these phenomena is the bond ordered wave phase between the spin density and charge density wave phases of the extended Hubbard model. See P. Sengupta, A.W. Sandvik, and D.K. Campbell, *Phys. Rev.* **B65**, 155113 (2002). Recent spin liquid examples in Hubbard models are described in M. Aidelsburger, M. Itala, S. Nascimbène, S. Trotzky, Y.A. Chen, and I. Bloch, *Phys. Rev. Lett.* **107**, 255301 (2011); H. Morita, A. Watanabe, and M. Imada, *J. Phys. Soc. Jpn.* **71**, 2109 (2002); Z. Meng, T. Lang, S. Wessel, F. Assaad, and A. Muramatsu, *Nature (London)* **464**, 847 (2010); and Chia-Chen Chang and R.T. Scalettar, *Phys. Rev. Lett.* **109**, 026404 (2012).